DESIGN AND MODELING OF TRAVELLING WAVE ELECTRODE ON ELECTROABSORPTION MODULATOR BASED ON ASYMMETRIC INTRA-STEP-BARRIER COUPLED DOUBLE STRAINED QUANTUM WELLS ACTIVE LAYER

Kambiz Abedi
Department of Electrical Engineering, Faculty of Electrical and Computer Engineering,
Shahid Beheshti University, G. C., Evin, Tehran, Iran

ABSTRACT

In this paper, a travelling wave electroabsorption modulators (TWEAMs) based on asymmetric intra-step-barrier coupled double strained quantum wells (AICD-SQW) active layer is designed and analyzed at 1.55 μm for the first time. The AICD-SQW structure has advantages such as very low insertion loss, zero chirp, large Stark shift and high extinction ratio in comparison with the intra-step quantum well (IQW) structure. For this purpose, the influence of the electrode width and ground metal separation on their transmission line microwave properties (microwave index, microwave loss, and characteristic impedance) and modulation bandwidth are analyzed.

KEYWORDS: *travelling wave electroabsorption modulator, aicd-sqw, microwave properties, modulation bandwidth.*

I. INTRODUCTION

Electroabsorption modulators (EAMs) are advantageous external modulators in high-speed optical communication systems due to low chirp, small size, high modulation efficiency, low driving voltage, high extinction ratio, wide modulation bandwidth and the capability to be integrated with other semiconductor devices. Improving the operation by overcoming the trade-off between bandwidth and device length, EAMs with travelling wave electrodes have been documented to be a good candidate [1-10]. Fig. 1 shows the principle of operation for a travelling-wave electroabsorption modulator. In a travelling-wave electrode configuration, the microwave signal is applied from one end of the optical waveguide and it co-propagates with the optical signal. At the output end of the waveguide, the microwave signal is terminated with a matching load such that there is little reflection from this end. Therefore, in a TW-EAM, the electrode is designed as a transmission line to distribute the capacitance over the entire device length [5]. This can increase the modulation efficiency while maintaining a large bandwidth. The bandwidth and the device length are only limited by the microwave loss at high frequencies, which includes propagation loss and source port reflection loss and the velocity mismatch between the optical signal and the microwave signal. Another limiting factor is the increased optical loss with a longer device, which is related to the optical signal-to-noise ratio of the modulated signal [3]. Due to waveguide dispersion, high frequency components will experience smaller characteristic impedance and hence higher reflection loss when launched from a 50 Ω driver [8-12]. In previous articles, we have proposed an asymmetric intra-step-barrier coupled double strained quantum well (AICD-SQW) structure based on the InGaAlAs material system that has advantages such as large Stark shift, very low insertion loss, zero chirp, high extinction ratio, and higher figures of merit in comparison with the IQW structure [13-17].

In this article, we have designed and analyzed a TWEAM based on asymmetric intra-step-barrier coupled double strained quantum wells at 1.55 μm optical wavelength for the first time. Design of TWEAM includes the reduction of electrical losses, velocity mismatch, and impedance mismatch. It

is therefore important to have control over parameters such as electrical propagation constant and characteristic impedance of the TWEAM transmission line electrode. Here we focus on the influence of the TWEAM transmission line electrode width and ground metal separation on their transmission line microwave properties such as microwave index, microwave loss, characteristic impedance and modulation bandwidth.

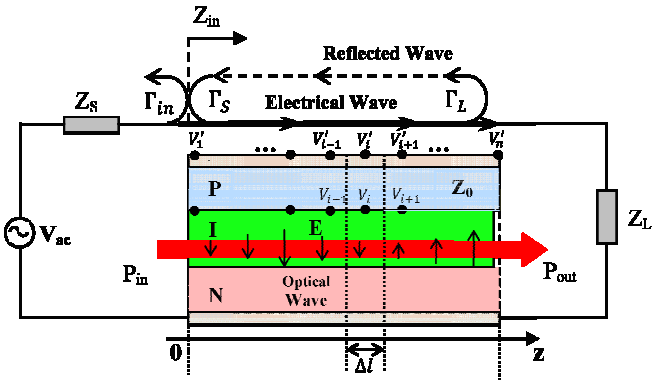

Figure 1. Principle of operation of TWEAM transmission line [14-15]

II. ACTIVE REGION OF TWEAM

A schematic illustration of the compositions and the thicknesses of the active region layers of TWEAM based on AICD-SQW structure are shown in Fig. 2 [13]. The figure also illustrates the direction of the applied electric field *F*.

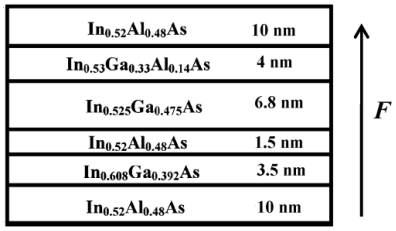

Figure. 2 Schematic of layers for AICD-SQW structure, Direction of applied electric field *F* is indicated as well

The undoped AICD-SQW structure has $In_{0.52}Al_{0.48}As$ barriers, which are lattice matched to the InP substrate, as well as one lattice-matched $In_{0.53}Ga_{0.33}Al_{0.14}As$ intra-step-barrier. The $In_{0.525}Ga_{0.475}As$ wide well is under 0.05% of tensile strain, and the $In_{0.608}Ga_{0.392}As$ narrow well is under 0.52% of compressive strain. The thickness of each of the two external barriers is 10 nm, while the thickness of the middle barrier is 1.5 nm. The thicknesses of the wide well, the narrow well and the intra-step-barrier are 6.8 nm, 3.5 nm and 4 nm, respectively. The middle barrier layer and strain amount of wells cause the electron and heavy hole wave functions are distributed dominantly in the wide and narrow wells, respectively. As a result, the insertion loss significantly decreases at zero electric field [13, 14].

III. FREQUENCY RESPONSE OF TRAVELLING WAVE ELECTROABSORPTION MODULATOR

TWEAMs are devices to modulate light waves corresponding to travelling electric fields along the electrode consisting of a transmission line. Because the absorption coefficient of TWEAMs is dependent on the electric voltage, the modulation of optical wave occurs by the absorption change due

to modulated electric signals. Fig. 3 shows the circuit model for a unit length of transmission line of TWEAM based on AICD-SQW active layer.

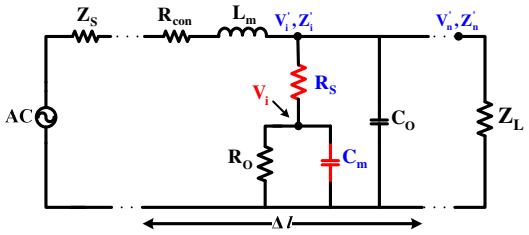

Figure 3. Circuit model for a unit length of transmission line of the TWEAM based on AICD-SQW active layer [14]

The small signal frequency response for TWEAM can be obtained as follows [11]:

$$\left|P_{ac}\right|^2 = \left| \sum_{i=1}^{n} \left(V_i e^{\,j\frac{\omega}{c_0} n_{o\_eff}\,(i-1)\Delta l}\,\Delta l \right) \right|^2 \qquad (1)$$

where V_i is the modulating voltage in i section. The voltage on the transmission line is the superposition of forward and backward travelling voltage waves that arise from reflections at the source and the load terminal, respectively. Eq. (1) can be developed analytically as follows [3]:

$$\left|P_{ac}\right|^2 = \left| \frac{1}{\left(\frac{R_s}{R_o} + 1 + j\,\omega R_s C_m\right)} \cdot \frac{V_0 Z_0 / (Z_s + Z_0)}{\left(1 - \Gamma_s \Gamma_L e^{-2\gamma_\mu L}\right)} \cdot \left[\frac{1 - e^{(-\gamma_\mu + j\beta_o)L}}{\gamma_\mu - j\beta_o} - \frac{\Gamma_L e^{-2\gamma_\mu L}\left(1 - e^{(\gamma_\mu + j\beta_o)L}\right)}{\gamma_\mu + j\beta_o} \right] \right|^2 \qquad (2)$$

where V_0 is the forward microwave voltage in the source transmission line, Z_0 is the characteristic impedance and γ_μ is the propagation constant of modulator transmission line. Γ_S and Γ_L are the modulator reflection coefficients at the source and load ports, respectively. ω is the microwave frequency, and $\gamma_\mu = \alpha_\mu + j\beta_\mu$, where α_μ is the microwave loss and $\beta_\mu = \omega/v_\mu$, is the wavenumber associated with the microwave phase velocity v_μ and $\beta_o = (\omega/c_0)\, n_{o\_eff}$ is the wavenumber associated with the optical phase velocity. The calculation of the small signal modulation response requires the knowledge of the optical index n_{o_eff} and the circuit model elements. The circuit elements can easily be extracted from the TWEAM transmission line microwave properties Z_0 (characteristic impedance) and γ_μ (propagation constant) [6], which are obtained via full-wave calculations of the given geometry.

IV. RESULTS AND DISCUSSION

In this section, we investigate the effects of the TWEAM transmission line electrode width (w_e) and ground metal separation (w_g) on their transmission line microwave properties such as microwave index n_μ, microwave attenuation α_μ, characteristic impedance Z_0 and modulation bandwidth. In this study, the thickness of the active layer is taken as 0.2064 μm. In order to improve the junction capacitance, we use a small intrinsic buffer layer, i-InP on top of the active layer with thickness of 0.2 μm. The width of the active layer, w_a is considered as 2 μm and modeling is performed for a wavelength of 1.55 μm. In the numerical modeling, the thicknesses of p- and n-mesa are taken as 1.7 μm and 1.5 μm, respectively. The corresponding geometry values and typical material data are in [14]. For our case study, we use data for the InP/InGaAsP material system according to published devices [13, 14]. Furthermore, the effective optical index, n_{o_eff} defines the optical speed, which should be known in the analysis of a travelling wave modulator. The calculated effective optical index using full-vectorial finite difference method is 3.512 [15].

Fig. 4 shows the calculated real part of characteristic impedance Re(Z_0) over frequency for different combinations of w_e and w_g. The real part of characteristic impedance draws near a constant level for frequencies above 10 GHz. This value is usually mentioned to as the modulator impedance. It can be observed that as the electrode width is increased, the real part of characteristic impedance value is reduced (Fig. 4a), but this value increases when the ground metal separation (w_g) is increased (Fig. 4b). With the change of the width of electrode, the circuit model elements R_{con}, L_m, and C_o are affected. Therefore, by widening the electrode, ohmic losses are reduced and the inductance L_m, decreases since the magnetic field path length changes. Furthermore, the area for the outer parasitic capacitance increases resulting in higher C_o. The junction capacitance C_m is not affected by changing the electrode width.

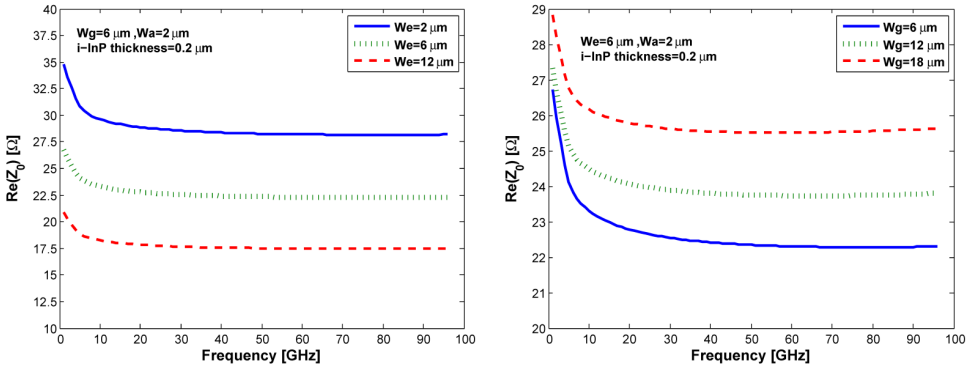

(a) (b)

Figure 4. Calculated real part of characteristic impedance Re(Z_0) versus frequency for different (a) electrode widths w_e and (b) ground metal separations w_g

Fig. 5 shows the calculated microwave index over frequency for different combinations of w_e and w_g. As the electrode width increases, the microwave index value decreases (Fig. 5a). The main effect of electrode width can be depicted best by considering an ideal transmission line without any losses. In this case microwave index is obtained as $n_\mu=c_0(L_mC_m)^{½}$. Increasing the width of electrode only decreases the inductance L_m in waveguide and decreases thereby the microwave index. Therefore, the microwave velocity increases. On the other hand, the microwave index value increases when the ground metal separation (w_g) is increased (Fig. 5b). Fig. 6 shows the calculated microwave loss over frequency for different combinations of w_e and w_g. It can be observed that as the electrode width is increased, the microwave loss value is reduced, but this value increases when the ground metal separations w_g is increased.

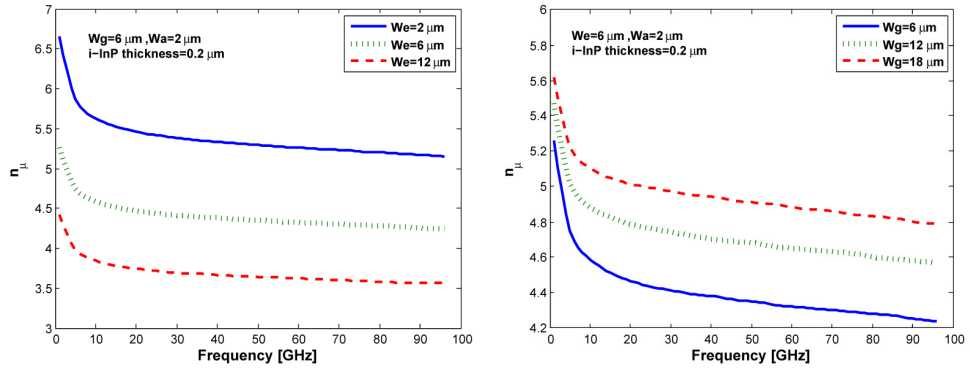

(a) (b)

Figure 5. Calculated microwave index versus frequency for different (a) electrode widths w_e and (b) ground metal separations w_g

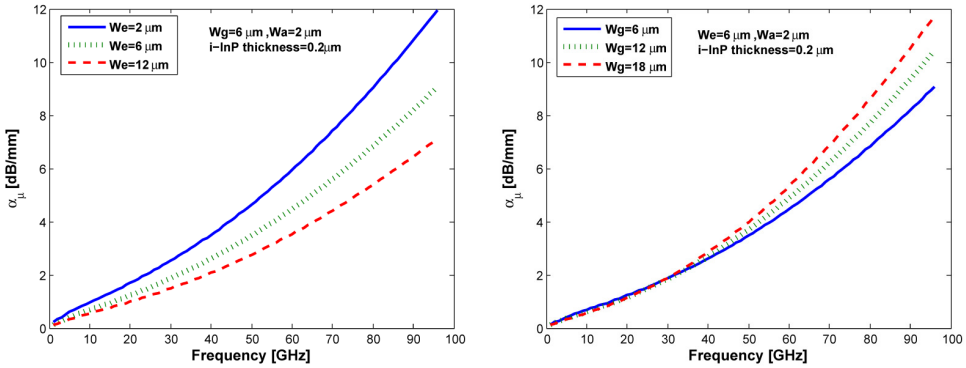

(a) (b)

Figure 6. Calculated microwave loss versus frequency versus frequency for different (a) electrode widths w_e and (b) ground metal separations w_g

In the design of the TWEAM, the microwave parameters n_μ, α_μ and Z_0 play important roles in determining the bandwidth of the modulator. The bandwidth of a high-speed modulator with a travelling-wave electrode is primarily limited by the velocity mismatch between the optical signal and the modulating microwave signal related to their modal indexes, n_{o_eff} and n_μ. For a high speed modulator, when phase velocity matching is achieved, the next limiting factor is the total microwave propagation losses α_μ. A design challenge for the TWEAM is a low characteristic impedance of 25 Ohm or below in the active waveguide, which causes reflections when driven by a 50 Ohm source and limits the modulation bandwidth. Therefore, low impedance terminations in the range of 12 to 35 Ohm are required to obtain the maximum bandwidth.

Fig. 7 shows the calculated frequency response of TWEAM based on AICD-SQW with different lengths and Z_L=25 Ω. The overall waveguide loss and velocity mismatch increase as the device length increases. The microwave loss and velocity mismatch reflect the decrease in optical modulation, as shown in the plot. The 3dB bandwidth for TWEAM based on AICD-SQW is about 83 GHz for 100 μm, 44 GHz for 200 μm and 22 GHz for 400 μm waveguide length, respectively.

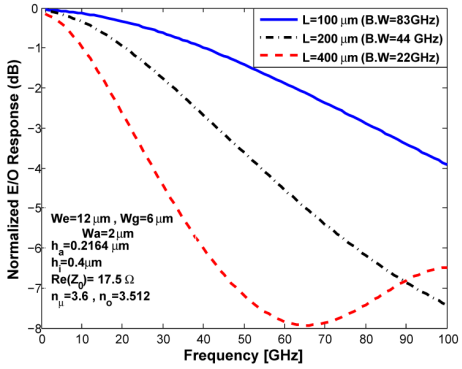

Figure 7. Frequency response for TWEAM based on AICD-SQW with different waveguide lengths

V. CONCLUSIONS

A travelling wave electroabsorption modulators (TWEAMs) based on asymmetric intra-step-barrier coupled double strained quantum wells (AICD-SQW) active layer was designed and analyzed at 1.55 μm for the first time. The AICD-SQW structure has advantages such as very low insertion loss, zero chirp, large Stark shift and high extinction ratio in comparison with the intra-step quantum well (IQW) structure. For this purpose, the influence of the electrode width and ground metal separation on their transmission line microwave properties (microwave index, microwave loss, and characteristic impedance) and modulation bandwidth were analyzed. The 3dB bandwidth for TWEAM based on

AICD-SQW is about 83 GHz for 100 μm, 44 GHz for 200 μm and 22 GHz for 400 μm waveguide length, respectively.

ACKNOWLEDGEMENTS

The author would like to express his gratitude to Professor V. Ahmadi and Dr. E. Darabi for the useful discussions.

REFERENCES

[1] G. L. Li, S. A. Pappert, P. Mages, C. K. Sun, W. S. C. Chang, and P. K. L. Yu, (2001) "High-Saturation High-Speed Traveling-Wave InGaAsP-InP Electroabsorption Modulator", *IEEE Photon. Technol. Lett.*, Vol. 13, No. 10, pp. 1076-1078.

[2] Y.-J. Chiu, H.-F. Chou, V. Kaman, P. Abraham, and J. E. Bowers, (2002) "High Extinction Ratio And Saturation Power Traveling-Wave Electroabsorption Modulator", *IEEE Photon. Technol. Lett.,* Vol. 14, No. 6, pp. 792-794.

[3] S. Irmscher, R. Lewen, and U. Eriksson, (2002) "InP-InGaAsP High-Speed Traveling-Wave Electroabsorption Modulators with Integrated Termination Resisrors", *IEEE Photon. Technol. Lett.,* Vol. 14, No. 7, pp. 923-925.

[4] J. Lim, Y.-S. Kang, K.-S. Choi, J.-H. Lee, S.-B. Kim, and J. Kim, (2003) "Analysis and Characterization of Traveling-Wave Electrode in Electroabsorption Modulator for Radioon- Fiber Application," *J. Lightwave Technol.,* Vol. 21, No. 12, pp. 3004-3010.

[5] G. L. Li, S. K. Sun, S. A. Pappert, W. X. Chen, and P. K. L. Yu, (1999) "Ultrahigh-Speed Traveling-Wave Electroabsorption Modulator - Design and Analysis," *IEEE Trans. Microw. Theory Tech.,* Vol. MTT- 47, pp. 1177-1183.

[6] S. Irmscher, R. Lewén, and U. Eriksson, (2002) "InP/InGaAsP high-speed traveling-wave electro-absorption modulators with integrated termination resistors," *IEEE Photon. Technol. Lett.*, Vol. 14, pp. 923–925.

[7] Y.-J. Chiu, S. Z. Zhang, V. Kaman, J. Piprek, and J. E. Bowers, (2001) "High-Speed Traveling-Wave Electroabsorption Modulators," *Symposium on Radio Frequency Photonic Devices and Systems II, 46th SPIE Annual Meeting, , San Diego, CA*.

[8] J. Piprek, Y.-J. Chiu, S. Zhang, J. E. Bowers, C. Prott, and H. Hillmer, (2003) "High-Efficiency Multi-Quantum-Well Electroabsorption Modulators," *Proc. ECS Symp. Integ. Optoelectron., Philadelphia, PA*.

[9] Y. J. Chiu, T. H. Wu, W. C. Cheng, F.J. Lin, and J.E. Bowers, (2005) "Enhanced performance in traveling-wave electroabsorption Modulators based on undercut etching the active-region," *IEEE Photon. Technol. Lett.,* Vol. 17, pp. 2065-2067.

[10] B. Liu, J. Shim, Y. Chiu, A. Keating, J. Piprek, and J. E. Bowers, (2003) "Analog characterization of low-voltage MQW traveling-wave electroabsorption modulators," *J. Lightwave Technol.,* Vol. 21, pp. 3011–3019.

[11] R. Lewén, S. Irmscher, and U. Eriksson, Microwave CAD Circuit Modeling of a Traveling-Wave Electroabsorption Modulator, IEEE Trans. Microwave Theory and Techn., Vol. 51, pp. 1117-1128, 2003.

[12] Y. L. Zhuang, W. S. C. Chang, and P. K. L. Yu, (2004) "Peripheral-coupled waveguide MQW electroabsorption modulator for near transparency and high spurious free dynamic range RF fiber-optic link," *IEEE Photon. Technol. Lett.,* Vol. 16, pp. 2033–2035.

[13] K. Abedi, V. Ahmadi, E. Darabi, M. K. Moravvej-Farshi, and M. H. Sheikhi, (2008) "Design of a novel periodic asymmetric intra-step-barrier coupled double strained quantum well electroabsorption modulator at 1.55 μm," *Solid. State. Electron.,* Vol. 53, pp. 312-322.

[14] K. Abedi, V. Ahmadi, and M. K. Moravvej-Farshi, (2009) "Optical and microwave analysis of mushroom-type waveguides for traveling wave electroabsorption modulators based on asymmetric intra-step-barrier coupled double strained quantum wells by full-vectorial method," *Opt. Quant. Electron.,* Vol. 41, pp. 719-733.

[15] K. Abedi, V. Ahmadi, E. Darabi, and M. K. Moravvej-farshi, (2008) "Numerical Analysis of Mushroom-type Traveling Wave Electroabsorption Modulators Using Full-Vectorial Finite Different Method," *International Journal of Optics and Photonics,* Vol. 2, pp. 9-17.

[16] V. Ahmadi, K. Abedi, and E. Darabi, (2007) "New Asymmetric Quantum Well Traveling-wave Electroabsorption Modulator with Very Low Insertion Loss and High Extinction Ratio," *Proc. of 9th International Conf. on Transparent Optical Networks ICTON*., pp. 251-256.

[17] K. Abedi, (2011) "An investigation of strain effect on saturation optical intensity in electroabsorption modulators based on asymmetric quantum wells," *Canadian Journal on Electrical and Electronics Engineering,* Vol. 2, No. 6, pp. 83-89.

Author

Kambiz Abedi was born in Ahar, Iran, in 1970. He received his B.S. degree from University of Tehran, Iran, in 1992, his M.S. degree from Iran University of Science and Technology, Tehran, Iran in 1995, and his Ph.D. degree from Tarbiat Modares University, Tehran, Iran, in 2008, all in electrical engineering. His research interests include design, circuit modeling and numerical simulation of optoelectronic devices, semiconductor lasers, optical modulators, optical amplifiers and detectors. Dr. Abedi is currently an Assistant Professor at Shahid Beheshti University, Tehran, Iran.